AGU ADVANCING EARTH AND SPACE SCIENCE

Geophysical Research Letters

RESEARCH LETTER
10.1029/2020GL090617

Increase in Compound Drought and Heatwaves in a Warming World

Sourav Mukherjee[1] **and Ashok Kumar Mishra**[1]

[1]Glenn Department of Civil Engineering, Clemson University, Clemson, SC, USA

Key Points:

- A significant increase in drought-related heatwave events and corresponding spatial extent is observed in the recent period
- The frequency, duration, and severity of compound drought and heatwave events have increased in five out of six continents
- The increasing pattern is spatially asymmetric, and greater amplification is noted across the Northern hemisphere due to recent warming

Supporting Information:

- Supporting Information S1

Correspondence to:
A. K. Mishra,
ashokm@g.clemson.edu

Citation:
Mukherjee, S., & Mishra, A. K. (2021). Increase in compound drought and heatwaves in a warming world. *Geophysical Research Letters*, *48*, e2020GL090617. https://doi.org/10.1029/2020GL090617

Received 30 AUG 2020
Accepted 1 DEC 2020

Abstract Compound drought and heatwaves can cause significant damage to the environment, economy, and society. In this study, we quantify the spatio-temporal changes in compound drought and heatwave (CDHW) events by integrating weekly self-calibrated Palmer Drought Severity Index (sc_PDSI) and daily maximum temperatures during the period 1983 to 2016. Multiple data products are used to examine the robustness of sc_PDSI in the compound event analysis. The results consistently suggest significant increases in drought-related heatwaves and affected global land area in recent (warmer) periods. Several regions across the globe witnessed rise in CDHW frequency (one to three events/year), duration (2–10 days/year), and severity. This increasing pattern is spatially asymmetric, and greater amplification is observed across the Northern hemisphere due to recent warming. Furthermore, the background aridity influences the spatiotemporal evolution of CDHW events. The results can be applied to minimize the impacts of extreme CDHWs in critical geographical regions.

Plain Language Summary The increase in global temperature has altered the spatio-temporal pattern of individual extreme events (e.g., drought and heatwave). However, a limited number of studies investigated their compound characteristics in terms of duration, frequency, severity, and spatial extent. This study explores the spatio-temporal changes in compound events that have a significant impact on health, agriculture, economy, and environment around the globe. The compound framework has a key advantage that it can capture the weekly droughts and heatwaves at daily time scale. The results can directly map the critical regions and reveal the dependence between two extreme events (i.e., drought and heatwaves). This study also examines the spatial asymmetry across the globe and the influence of background aridity on compound extremes in a warming climate. This analysis can be extended to inform stakeholders where the coevolution of these extreme events is likely to be higher under climate change. The results of this analysis will aid forecasting efforts and help to improve hazard preparedness and mitigation strategies for the vulnerable regions of the globe.

1. Introduction

Compound drought and heatwave (CDHW) events have garnered much attention in recent decades (Fink et al., 2004; Leonard et al., 2014; Mukherjee et al., 2020; Sutanto et al., 2020; Zscheischler et al., 2018). These CDHW events often impact socio-ecological systems (Mukherjee et al., 2020), which includes wildfires (Sutanto et al., 2020; Witte, 2011), massive heat-related deaths (D'Ippoliti et al., 2010; Mitchell et al., 2016), and loss of crop yield (Lu et al., 2018; Zampieri et al., 2017). Many regions around the world experienced CDHW events during the summer months of 2003, 2010, 2015, and 2018 in Europe and western Russia (Fink et al., 2004; Ionita et al., 2017; Liu et al., 2020; Witte, 2011); 2012–2014 in the USA (Diaz & Wahl, 2015; Griffin & Anchukaitis, 2014; Williams et al., 2015); 2013 in Australia (Cowan et al., 2014; Lewis & Karoly, 2013); 2006, 2009–2010, and 2014 in Southwestern and Northern China (Barriopedro et al., 2012; H. Wang & He, 2015; X. Wu et al., 2019; Ye et al., 2019).

The evolution of drought and heatwaves are controlled by a variety of land surface fluxes (Mishra & Singh, 2010), and their spatial patterns are heterogeneous due to the regional differences in precipitation, temperature anomalies, and other hydrological changes (Chen et al., 2013; Konapala & Mishra, 2020; Kumar et al., 2016; Mishra & Singh, 2010; Z. Wu et al., 2012). Besides, these land surface fluxes are influenced by the background aridity, anthropogenic factors, and large-scale changes in climate patterns (Fu & Feng, 2014; Karl & Trenberth, 2003; Meehl et al., 2004; Mukherjee et al., 2020; Sankarasubramanian et al., 2020).

Numerous studies have investigated CDHW events (Mukherjee et al., 2020) based on different combinations, such as monthly precipitation and temperature anomalies (Hao et al., 2018a); Standardized Precipitation Index and temperature anomalies (Kong et al., 2020; Mazdiyasni & AghaKouchak, 2015); precipitation deficit and potential evapotranspiration (Manning et al., 2018); and temperature anomalies and precipitation deficit (Lu et al., 2018). Nevertheless, the CDHW event estimation framework applied in these studies can be further improved in the context of the timescale as well as the type of indicators used to quantify drought and HWs (Miralles et al., 2019; Mukherjee et al., 2020; Teuling et al., 2013).

While many studies investigated compound extremes, this study further complements previous studies in three different ways. First, we applied a framework to estimate the frequency, duration, and severity of CDHW events by integrating weekly drought and daily HW information, which was neglected in earlier studies. This framework can overcome the limitations arising from the difference in the temporal evolution of heatwaves (i.e., daily to weekly scale) and droughts (i.e., weekly to monthly scale) (Mukherjee et al., 2020). Second, the spatial asymmetry of the temporal evolution of CDHW events is investigated for the first time on a global scale. Third, although background aridity plays a vital role in the development of drought and heatwaves, its potential influence on the evolution of CDHW events in different climate regimes (arid, transitional, and humid) remains largely unexplored.

The overall objective of this study is to quantify the spatiotemporal changes in the CDHW events at a global scale based on the following research questions: (a) how does the recent increase in temperature influence the CDHW events; (b) Is there a significant increase in the proportion of HW days coinciding with the extreme drought conditions? (c) to identify the regions that show a greater increase in the characteristics of CDHW events, and examine if there is spatial asymmetry associated with such growth at the global and hemispherical scale? (d) whether the background aridity controls the increase in CDHW characteristics at regional to the continental scale; and (e) whether these results are consistent across different data sets. This study is structured as follows. Section 2 describes the data and methodology used in the study. Section 3 provides results and discussion, followed by the summary and conclusions in Section 4.

2. Methods

2.1. Data

We use daily precipitation (P) data set obtained from the Global Precipitation Climatology Center (GPCC) (http://gpcc.dwd.de/), available at 1° spatial resolution for the period 1983–2016. GPCC precipitation data set is relatively consistent across the globe (Sun et al., 2018), therefore, it is expected to provide spatially robust estimates of CDHW characteristics. Available water content (AWC) is obtained from a soil texture-based global water-holding-capacity map produced by Webb et al. (2000), and extracted at 1° spatial resolution. Daily maximum and minimum 2 m air temperature (T_{max}, and T_{min}) data set is retrieved from the Climate Prediction Center (CPC) (https://www.esrl.noaa.gov/psd/; available at 0.25° spatial resolution) for the period, 1983–2016. Humid, transitional, and arid regions are identified based on the potential evaporation (Ep) data obtained from the European Centre for Medium-Range Weather Forecasts Reanalysis 5 (ERA5; https://cds.climate.copernicus.eu/cdsapp#!/home; available at 0.25° spatial resolution) at hourly time-steps for the same period. The data sets from the ERA5 potentially supersede other reanalysis products by its high spatial and temporal resolution. Additionally, we also use daily precipitation, T_{max} and T_{min} data from the ERA5 and T_{max} and T_{min} data from Berkeley Earth Surface Temperature Project (BE; http://berkeleyearth.org/data-new/) to investigate data related inconsistencies. All data sets are regridded at 1° spatial resolution by applying the bilinear interpolation scheme to make it consistent with the GPCC Precipitation data set.

2.2. Estimation of CDHW Event Characteristics

The summer CDHW events are calculated by integrating heatwave and drought information. In this study, the drought events are derived based on the weekly self-calibrated Palmer Drought Severity Index (sc_PDSI), and HW events are derived based on the abnormally high-temperature anomalies observed for three or more consecutive days. Besides, considering possible epidemiological significance (Keellings & Waylen, 2014), two successive HW events are considered independent if separated by a minimum of four days,

otherwise clustered into a single event. The sc_PDSI is calculated based on the methodology proposed by Wells et al., 2004. This procedure includes weekly total precipitation, weekly mean temperature (average of T_{max}, and T_{min}), and AWC in the energy-budget framework as inputs for deriving sc_PDSI. In addition, this methodology employs the potential evapotranspiration estimated using Thornthwaite's method (Thornthwaite, 1948). In our analysis, the sc_PDSI is derived utilizing the climate characteristics calibrated based on the whole period, 1983–2016.

The CDHW events are estimated based on the time periods when a HW coincides with the extreme drought weeks (Mukherjee et al., 2020). An extreme drought week is identified when the sc_PDSI magnitude falls below the 10th percentile of the weekly values during the study period (Mukherjee et al., 2020). The daily temperature anomalies are calculated for each location, separately, based on the corresponding 90th percentile of daily maximum temperature observed in the extended summer seasons (May-October in the northern hemisphere, and November-April in the southern hemisphere) from 1983 to 2016. The concept of identifying HW event is analogous to previous studies conducted for different parts of the Globe (Fischer & Knutti, 2015; Meehl & Tebaldi, 2004; Perkins et al., 2012; Unkašević & Tošić, 2013).

In this study, CDHW events are characterized by three metrics: (a) CDHW frequency ($CDHW_f$), defined as the average number of annual CDHW events during the study period; (b) CDHW days ($CDHW_d$), defined as the total number of event days observed for a given year; and (c) CDHW severity ($CDHW_s$), which is calculated based on the cumulative sum of the daily severity values obtained over the consecutive days of the CDHW events. The daily severity is estimated as the product of the daily standardized values of maximum temperatures and the scPDSI value observed in the coinciding extreme drought week. A description of the methodology used in the estimation of CDHWs is provided in A.1. of the Supporting information.

3. Results

3.1. Changes in the CDHW Events

We investigate the annual changes in proportion of CDHW events and global land area witnessing these events during the study period, 1983–2016. The proportion of CDHW events for a specific year is calculated based on the ratio (% change) between the total number of CDHW and HW events occurring at any given location. Hereafter, this ratio (%) is referred to as $CDHW_r$. The $CDHW_r$ estimation allows us to investigate interannual changes in the proportion of HW events that coincide with the extreme drought weeks.

Based on this concept, the time series of $CDHW_r$ are constructed for each grid location and subsequently averaged over the globe. The interannual trends in the global $CDHW_r$ are estimated and compared between the whole period (1983–2016), past period (1983–1999), and the recent warmer period (2000–2016) to investigate the potential contribution of recent warming. The criteria for selecting the past and recent warmer period is discussed in A2 of the Supporting Information. This criterion is evaluated based on the summer mean of daily T_{max} anomalies in the CPC, BE, and ERA5 data sets, as illustrated in Figure S1. It can be observed that the period from 2001 to 2016 was considerably warmer than the preceding period, 1983–2000. Notably, the temporal pattern exhibited by the magnitude of these anomalies shows a close agreement among all the three data sets (Figure S1). Such consistencies among the three (potentially) different temperature data sources can minimize the possibility of uncertainties in the analysis.

In this study, the trends are determined by employing the Sens's slope estimator, and the statistical significance of the trends is tested based on the MK test (Kendall, 1948; Mann, 1945) at 95% confidence level (see A3 of the Supporting Information). Similarly, we also examine the interannual changes in the percentage of global land area (estimated as the percentage of land area within the grid cells weighted by the cosine of their latitudes) that witnessed a CDHW event during these three periods. Even across different quality-controlled data sets, trends can often vary substantially, even if year to year variability is congruent and especially for variables with larger uncertainties like precipitation. Specifically, PDSI estimates of drought trends depend critically on the precipitation data sets being used (Mukherjee et al., 2018; Trenberth et al., 2014). To investigate data related inconsistencies, these changes are analyzed based on three different combinations of data sets: (1) precipitation from GPCC and temperature from CPC (GPCC-CPC), (2) precipitation from GPCC and temperature provided by Berkeley Earth Surface Temperature Project (GPCC-BE), and (3) precipitation and temperature both from ERA5. These changes are illustrated in Figure 1.

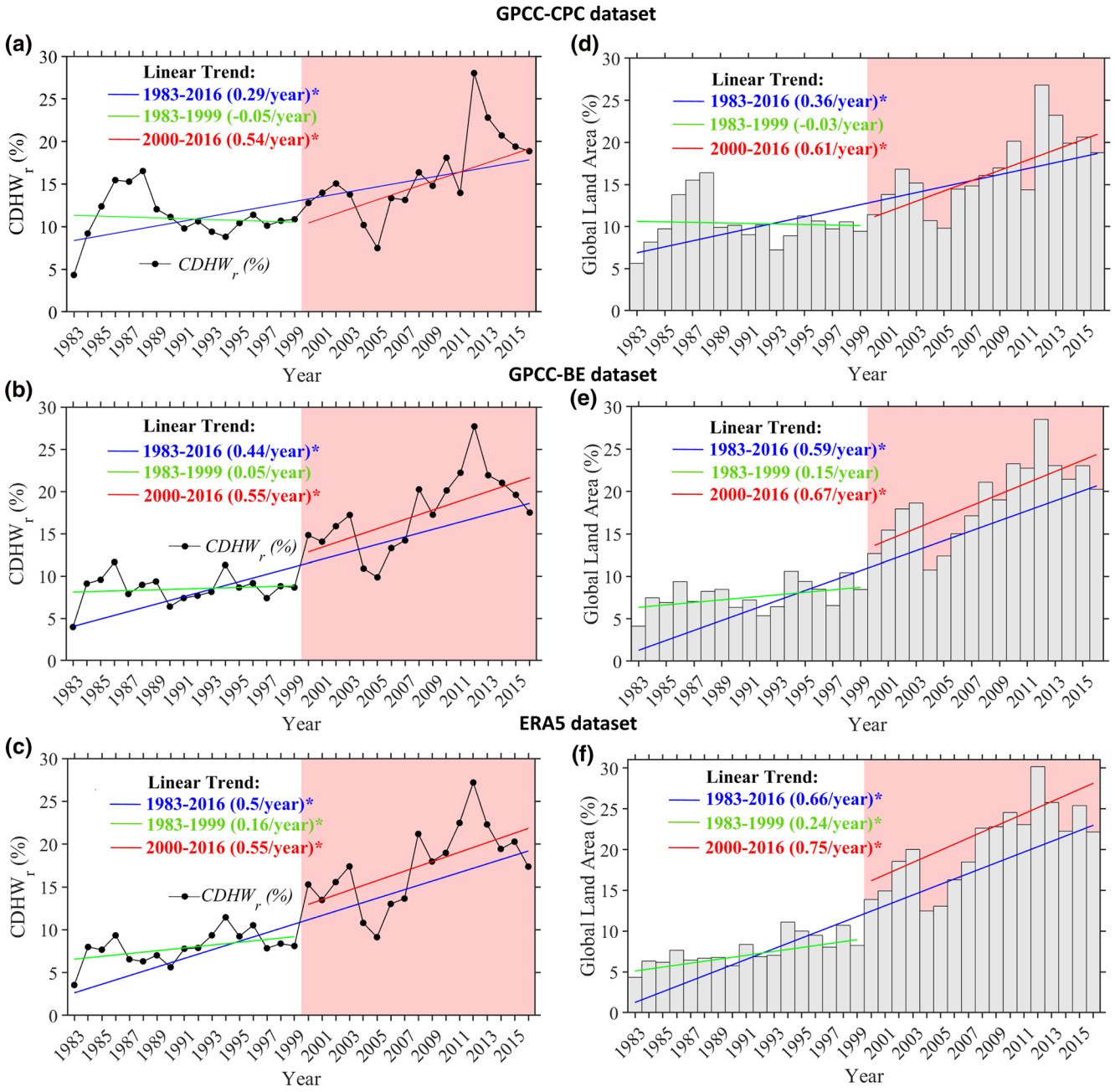

Figure 1. (a–c) Linear and scatter plots show the annual timeseries of globally averaged $CDHW_r$ (%) based on (a) GPCC-CPC data set, (b) GPCC-BE data set, (c) ERA5 data set, and (d–f) bar-plots illustrate the percentage of global land area) affected by the CDHW events each year during the whole study period, 1983–2016 (%) based on (d) GPCC-CPC data set, (e) GPCC-BE data set, (f) ERA5 data set. Linear annual trends in $CDHW_r$ and in the global land area are estimated based on the Sen's slope estimator, and statistical significance in trends are determined based on the MK test for the whole study period (1983–2016), past period (1983–1999), and recent warm period (2000–2016). The numbers in the bracket indicate the estimated slope, and the asterisks denote statistically significant trends (at 95% confidence level). CDHW, compound drought and heatwave; CPC, Climate Prediction Center; ERA5, European Centre for Medium-Range Weather Forecasts Reanalysis 5; GPCC, Global Precipitation Climatology Center.

The global averages of $CDHW_r$ depict a significant (at 95% confidence interval) increasing trend during the whole period, 1983–2016, and in the recent warmer period, 2000–2016 across all three data sets (Figures 1a–1c). The magnitude of the estimated slope suggests a 0.54%–0.55% increase in $CDHW_r$ per year during the recent warmer period in all three data sets, a rate of increment almost double of that (0.29% per year) observed during the whole period in the GPCC-CPC data set. The relative cooler past period, 1983–1999, on

the other hand, shows a decreasing trend in the $CDHW_r$ values in the GPCC-CPC data set and a negligibly low rate of increase in the GPCC-BE and ERA5 data set. These results indicate a consistent and significant influence of warming on the recent increases in the drought-related HW events across the globe. The percentage of land area that witnessed a CDHW event (shown in bar plots) has also increased simultaneously in the recent warmer period in all three data sets (Figures 1d–1f). Both $CDHW_r$ magnitude and spatial extent of CDHW events are found to be the maximum during the year 2012 across all three data sets. Almost 28% of the total HW events occurred during extreme drought weeks in the year 2012 (Figures 1a–1c), affecting 27%–29% of the global land area (Figures 1d–1f).

3.2. Spatiotemporal Changes in CDHW Event Characteristics

3.2.1. Global and Hemispherical Changes

The spatiotemporal patterns of the CDHW characteristics are quantified based on three metrics, such as the $CDHW_f$, $CDHW_d$, and $CDHW_s$ for the recent warmer period, 2000–2016 with respect to the relatively cooler past period, 1983–1999. The spatial maps for the $CDHW_f$, $CDHW_d$, and $CDHW_s$ for the two periods are presented in Figures S2–S4, respectively, corresponding to the three combinations of data sets chosen for the study. The corresponding changes between the two time periods are quantified by subtracting the magnitude of CDHW characteristics between recent and past periods (Figure 2).

In most of the regions, a relatively higher frequency ($CDHW_f$) of CDHW events (one to three more events per year) are observed during the recent period (Figures 2a–2c). These increases are consistent in all three data sets (GPCC-CPC, GPCC-BE, and ERA5) over the United States, the Amazon basin, central and northern Europe, west and central Asia, and most parts of Australia. Similarly, these regions witness a relative increase in the magnitude of two other CDHW metrics, $CDHW_d$, and $CDHW_s$ during the recent period. The CDHW events in these locations are characterized by 2–10 days/year increase in $CDHW_d$ (Figures 2f) and 6–30 per event/per year increase in $CDHW_s$ (Figure 2i) during the recent period (2000–2016). Interestingly, the results corresponding to the GPCC-BE and ERA5 data sets show more consistent spatial patterns that differ in the GPCC-CPC data set over Western South America, North of Northern America, India, China, and most of Africa.

Our results suggest that 58%–73%, 60%–75%, and 56%–65% of land area in the NH show an increase in $CDHW_f$, $CDHW_d$, and $CDHW_s$, respectively, whereas 51%–74%, 54%–76%, and 49%–65% of the land area witnessed such increase over the SH. These results indicate the presence of a spatial asymmetry, with a higher percentage of area in the NH being affected by the more extended duration and more severe CDHW events as compared to the SH in the recent period as a result of warming. Importantly, these results are robust across the three different combinations of data sets employed in the analysis.

3.2.2. Latitudinal Variations

The latitudinal variations of CDHW metrics are examined to further investigate their spatially asymmetric behavior due to warming at the global scale (Figure 3, and Figure S5). In this study, the latitudinal variations (represented by the heatmaps) are captured at 1° intervals between −54.5°N and 65.5°N. Figure S5 depicts these variations for $CDHW_f$, $CDHW_d$, and $CDHW_s$ during individual years within the whole study period based on each of the three different combinations of data sets. The latitudinal variation of the CDHW metrics are also compared among the recent and past period based on their corresponding 17-year averages and associated interannual trends (illustrated by the line plots in Figure 3. The latitudes with statistically significant (at 95% confidence level) trend are indicated by the "square" symbols. The magnitude of the trends and significant directions (increasing/decreasing) are estimated based on the Sens's slope estimator and the MK test (Kendall, 1948; Mann, 1945), respectively (see A3 in the Supporting Information). This analysis can reveal the temporal shifts and rate of change of CDHW metrics across the latitudes as an impact of warming.

The heatmaps show considerable spatial asymmetry for each of the CDHW metrics across the latitudes that seem to be characterized by a skewed temporal pattern in response to the warming climate (Figure S5) in all three data sets. This asymmetric behavior is prominent across the mid-latitude regions (tropical and extratropical regions) of both hemispheres, with relatively more consistent patterns observed in the northern (southern) hemisphere in the GPCC-CPC (GPCC-BE) and ERA5 data set. Peak magnitudes of $CDHW_f$,

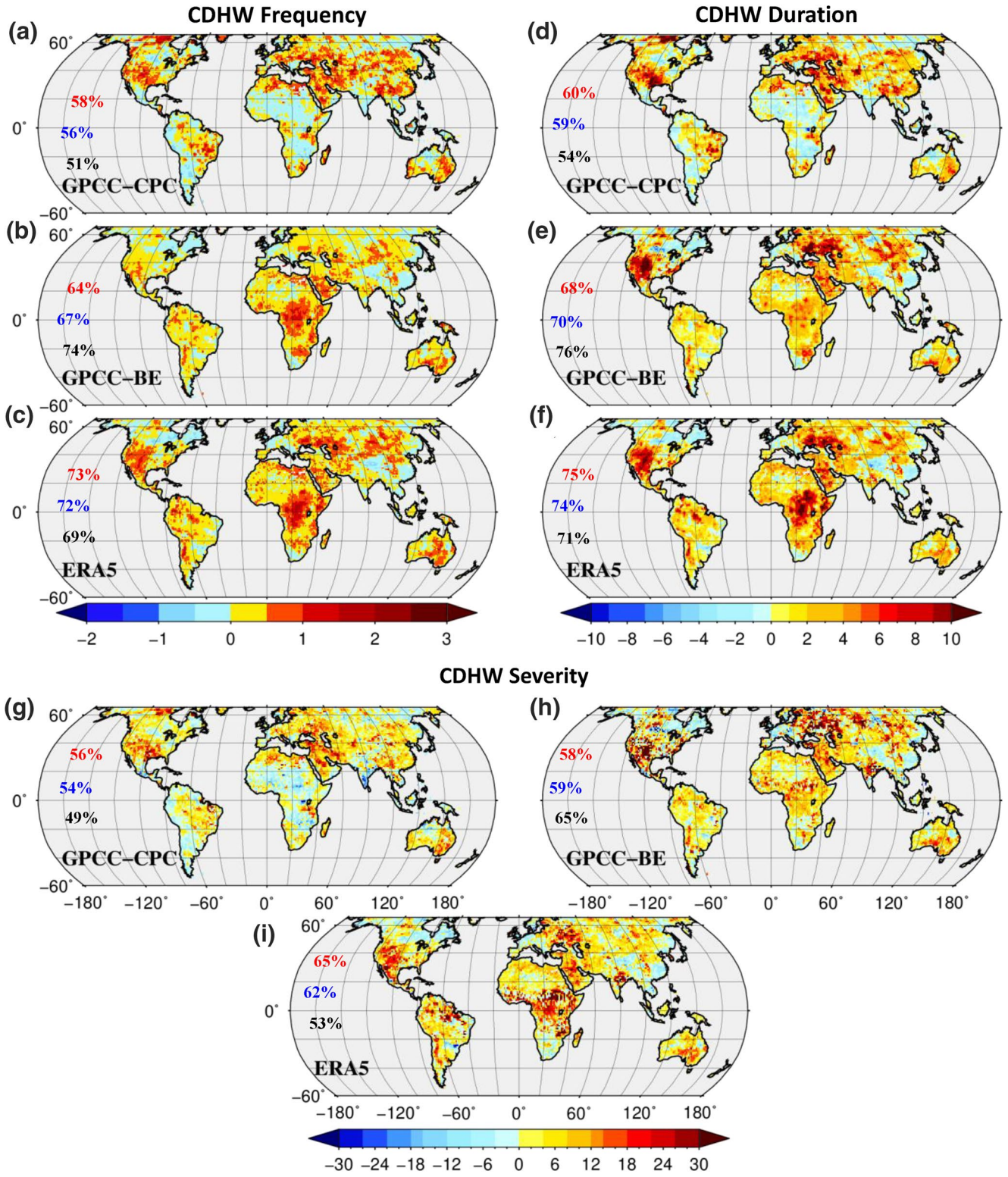

Figure 2. Spatial map showing the changes in (a–c) $CDHW_f$ between two time periods (recent, 2000–2016 minus past, 1983–1999) based on (a) GPCC-CPC data set, (b) GPCC-BE data set, (c) ERA5 data set, (d–f) same as in (a–c) but for the $CDHW_d$ (days/year), and (g–i) same as in (a–c) but for the CDHWs (per event/year). The numbers illustrated in (a–i) represent the percentage of area affected by an increase in the corresponding CDHW metrics for the NH (red), globe (blue), and SH (black). CDHW, compound drought and heatwave; CPC, Climate Prediction Center; ERA5, European Centre for Medium-Range Weather Forecasts Reanalysis 5; GPCC, Global Precipitation Climatology Center.

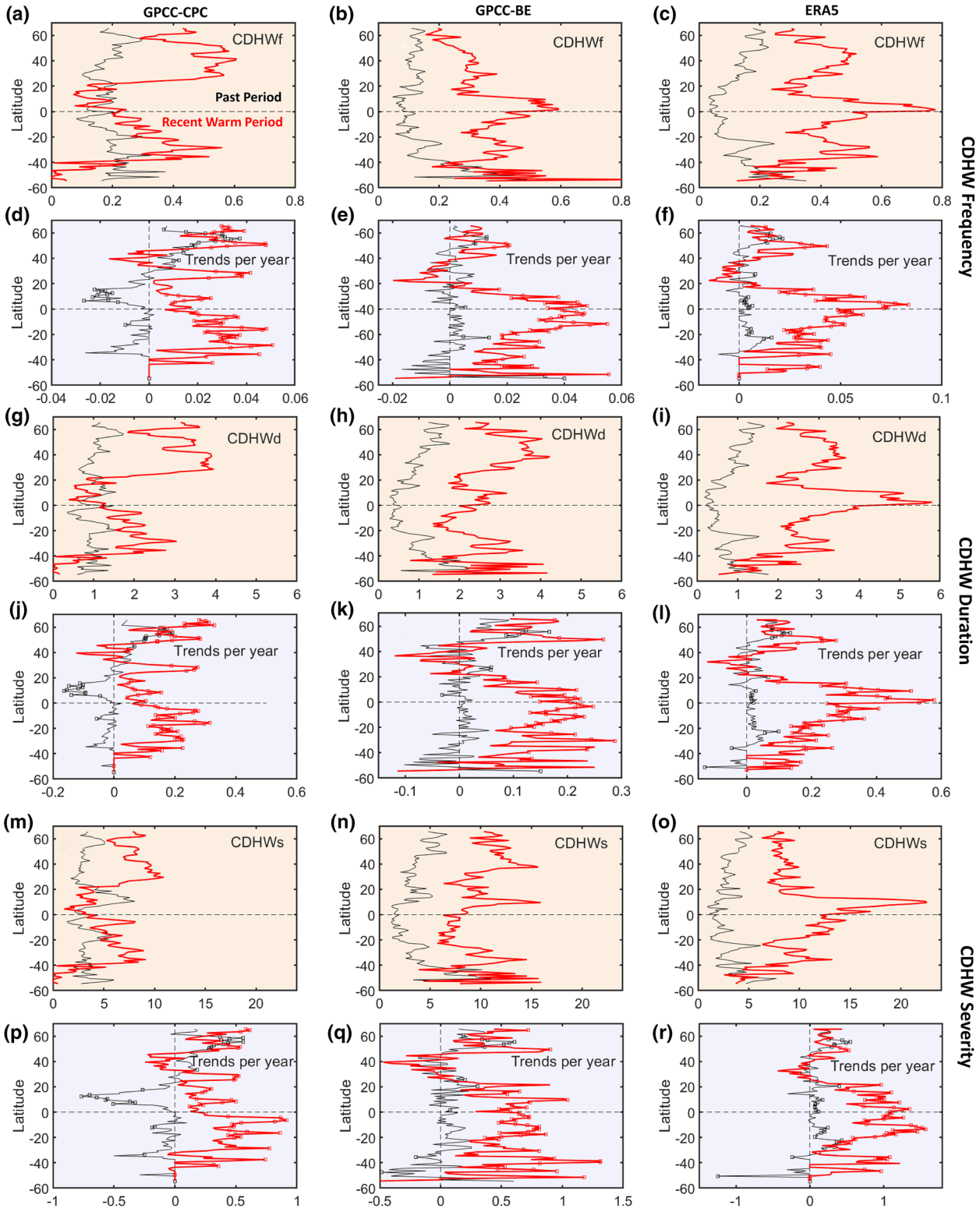

Figure 3. (a–c) Line plots showing the latitudinal variation in the past period (1983–1999; in black) average and recent warmer period (2000–2016; in red) average of $CDHW_f$ (events/year) based on (a) GPCC-CPC data set, (b) GPCC-BE data set, (c) ERA5 data set, (d–f) interannual trends in CDHW characteristics for the past (in black) and recent warmer period (in red) based on the three individual data sets, (g–l) same as in (a–f) but for $CDHW_d$ (days/year), and (m–r) same as in (a–f) but for the CDHWs (per event/year). The square symbols mark the latitudes showing statistically significant trends in the interannual variation of the CDHW metrics. CDHW, compound drought and heatwave; CPC, Climate Prediction Center; ERA5, European Centre for Medium-Range Weather Forecasts Reanalysis 5; GPCC, Global Precipitation Climatology Center.

$CDHW_d$, and $CDHW_s$ in the past period are only limited to a short time period (1987–1989) clustered over the extratropical region (between −30°N and −54.5°N) of the SH. However, such momentary amplifications can be attributed to sudden increases in hot and dry events across South America influenced by natural climate variability (Lough, 1995). On the other hand, the CDHW metrics have amplified considerably during the (relatively warmer) recent period, 2000–2016, in both hemispheres.

In all three data sets, the CDHW metrics are observed to vary substantially between NH and SH, and the maximum difference is observed during 2012 (Figure S5). During this year, the peak magnitudes of CDHWf (one to two events), CDHWd (7–12 days), and CDHWs (20–25 per event) were observed mostly across the mid-latitude regions (21.5°N–65.5°N) located in the NH. This particular latitude range encompasses the extratropical regions of Europe, Asia, and North America. These specific regions witnessed unprecedented heat events accompanied by persistent droughts mostly triggered by anthropogenic warming (Griffin & Anchukaitis, 2014; Mitchell et al., 2016; Williams et al., 2015). The magnitude of the 2012 European heatwave is found even to exceed that of the 2003 summer heatwave events considered to be one of the most deadly event in the continent (Mitchell et al., 2016). On the other hand, the high amplifications in the SH are clustered over the years 2013–2016 across the latitudes −4.5°N to −45.5°N. The amplified signals of the 2013 CDHWs emerging over the SH can be associated with the unprecedented Australian summer heat (considered as the "angry summer") attributed to anthropogenic warming (Lewis & Karoly, 2013).

The latitudinal variation of the average CDHW metrics during the past and the recent period provides a more detailed narrative on the association between the spatially asymmetric amplification and the warming climate (Figure 3). The amplification in the recent warmer period is found to be higher over the NH as compared to the SH in all three data sets. More importantly, the broad range in which the minimum and maximum magnitude of the CDHW metrics vary across the latitudes has increased substantially in the recent period in both NH and SH. On the other hand, in all three data sets, this range is found to be relatively smaller and consistent in the past period, which amplifies uniformly across the tropical and extratropical regions. This indicates a higher spatial asymmetry in the recent warmer period relative to the cooler past period in the respective hemispheres. However, the amplifications noted across the equatorial region are overwhelming in the GPCC-BE, and ERA5 data set that substantially differs from that observed in the GPCC-CPC data set. This highlights the potential uncertainties associated with the use of different temperature data set in the region.

We further investigated the rate of increase in the spatial variation of CDHW characteristics based on the past and recent periods (Figure 3). Although a stable behavior can be observed in the past period, more dynamics in terms of latitudinal symmetry is distinctly visible during the recent period. During the past period, a greater number of latitudes located in the NH witnessed significantly higher positive interannual trends; however, the pattern reversed diametrically during the recent warmer period as considerably higher trends are observed over a continuous stretch of the SH, particularly between −1°N and −30°N latitudes across all the three data sets. Overall, these results indicate major spatiotemporal asymmetry and heterogeneity associated with the rate of change in CDHW characteristics. However, both the mean magnitudes and trends associated with the recent warmer period are significantly higher in the ERA5 data set as compared to both GPCC-CPC, and GPCC-BE data sets. This may be linked to the uncertainties associated with the use of different data sets that emerge in the reanalysis-based estimates of CDHW metrics under warmer conditions.

3.3. Effect of Background Aridity at Continental Scale

We investigated the possible role of aridity on the asymmetric (heterogeneous) behavior of CDHW metrics. The background aridity has a potential influence on the evaporation and land-atmospheric interactions (McVicar et al., 2012; Mukherjee et al., 2020; Sankarasubramanian et al., 2020; Seneviratne et al., 2010), that directly controls the drought and heatwaves. The influence on evaporation is primarily defined based on the concept of water-limited and energy-limited regimes (Budyko & Mikhail, 1971; D. Wang & Tang, 2014). Water-limited evaporation is dominant in the arid regimes, and it is mainly controlled by the variation in soil moisture. On the other hand, the energy-limited evaporation is common in humid regimes and regulated by the availability of surface energy. To investigate the potential influence of such type of control (water-limited and energy-limited) over the spatiotemporal changes in the CDHW events in a warming

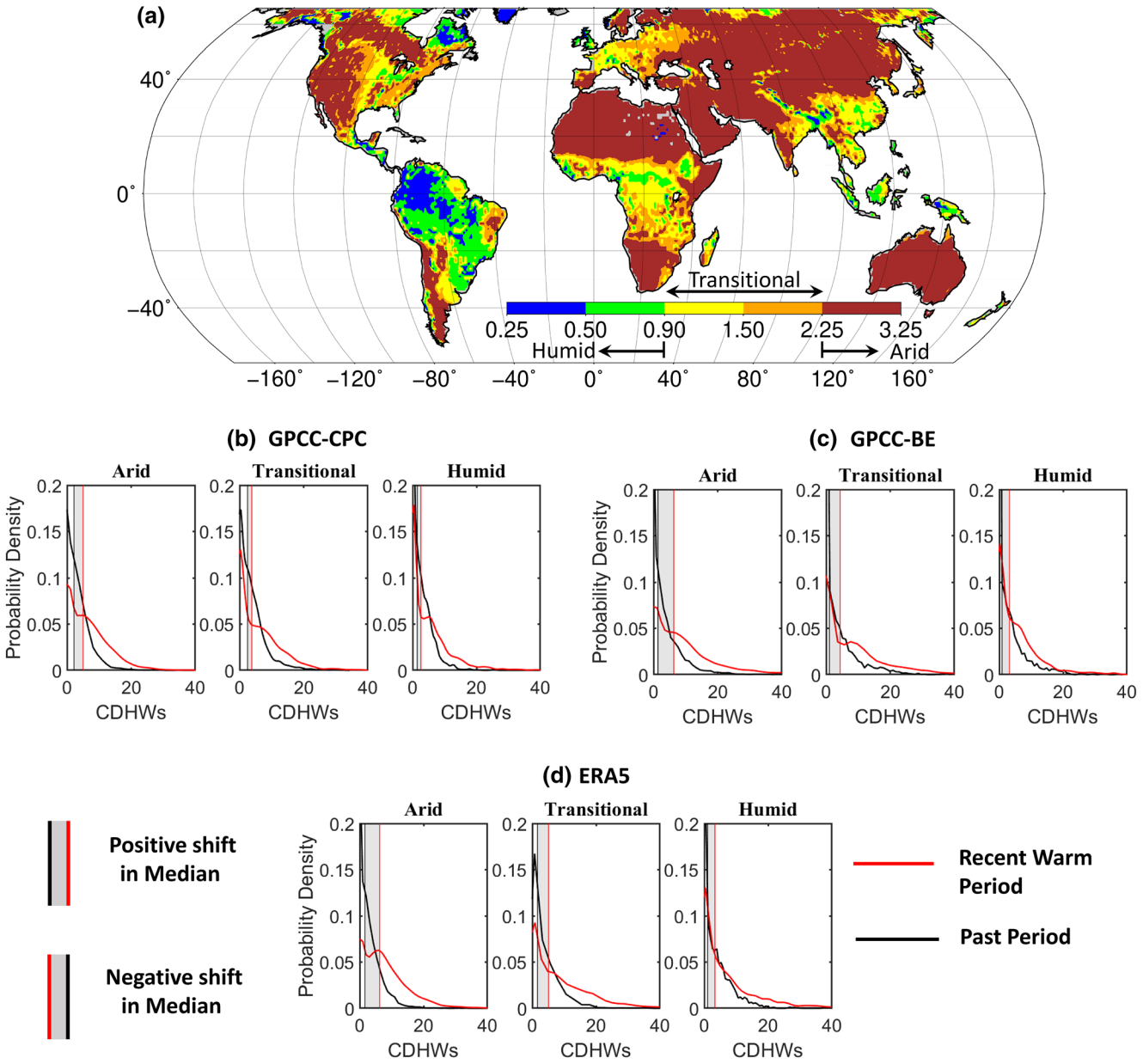

Figure 4. (a) Spatial map showing the arid, transitional, and humid regions identified based on the Aridity Index for the climatological period, 1983–2016, (b–d) Probability density of Past, 1983–1999 period (black), and recent warm, 2000–2016 period mean CDHWs (per event per year) for the arid, transitional, and humid regions of the Globe based on (b) GPCC-CPC, (c) GPCC-BE, and (d) ERA5 data sets.

climate, we examine the CDHW metrics in the arid, transitional, and humid regimes located in six different continents across the globe.

In this study, the global arid, transitional, and humid regimes are identified based on the aridity index (*AI*) (Barrow, 1992). The *AI* is calculated based on the ratio between the climatological annual-average potential evaporation and precipitation (Ep/P), which represents the dryness/desertification characteristic over a region (Cherlet et al., 2018; Greve et al., 2019). The global map of the arid ($AI > 2.25$), transitional ($0.9 < AI \leq 2.25$), and humid ($AI \leq 0.9$) regimes derived based on the climatological period of 1983–2016 (Zheng et al., 2019) is shown in Figure 4a. To examine if the warming climate has a significant influence on the spatiotemporal changes in the CDHW events over these regimes, we investigate the statistically significant change in the spatial distribution and shift in the median value of the CDHW metrics. To investigate

if these changes are dependent on the choice of data sources, the analysis is performed based on the three different combinations of data sets separately. Firstly, the 17-year mean magnitudes of the CDHW metrics (CDHWf, CDHWd, and CDHWs) are calculated for the past (1983–1999) and recent (2000–2016) periods, separately. Finally, the spatiotemporal changes between the past and relatively warmer recent periods are investigated by comparing the probability density function of mean CDHW metrics ($CDHW_f$, $CDHW_d$, and $CDHW_s$) for three different *AI* regimes. The probability density functions are generated by using appropriate non-parametric kernel density estimators. Figures 4b–4d, Figures S6b–S6g, S7b–S7h, and S8b–S8h present the probability density functions for the $CDHW_s$, $CDHW_f$, and $CDHW_d$ obtained for each of the three different regimes based on the globe and six continents.

The statistically significant change in the spatial distribution and shift in the median value of CDHW metrics are investigated for the recent period relative to the past period by using the two-sample Kolmogorov-Smirnov test, and Wilcoxon rank-sum test (see A.4 in the Supporting Information), respectively. In all three data sets, the spatial pattern of the mean CDHW metrics across the globe exhibit a significant (at 95% confidence level) positive shift in the median and the overall distribution during the recent period in all three regimes (arid, transitional, and humid), however a relatively more prominent positive shift in the median can be observed across the arid regimes (Figures 4b–4d).

Furthermore, a consistent increase in the CDHW metrics in the recent period is notable for the arid and transitional regimes of North America, Europe, Australia, and arid regimes of Asia (Figures S6–S8). Nevertheless, considerable spatially heterogeneity among the climate regimes as well as across the continents can be noted across the data sets for the two time periods. The inter-continental heterogeneities are notable among Africa and South America relative to the rest of the continents in the GPCC-CPC data sets. Even changes in CDHW metrics in the GPCC-CPC data set across the humid regimes of Europe, North America, and Asia are diametrically opposite to those in the ERA5, and GPCC-BE data sets. Such notable inconsistencies across the humid regions may arise due to the uncertainties in temperature, specifically between the GPCC-CPC and GPCC-BE data sets. This can be explained by the higher sensitivity of evaporation in energy-limited conditions to changes in temperature (Miralles et al., 2019; Seneviratne et al., 2010). As such, more significant variability in the results is noted across the humid equatorial regions such as in South America and Africa.

Overall, our results are independent of the choice of data sets across significant regions and indicate an increasing influence (control) of aridity on CDHW events during the recent period (2000–2016) compared to the past (1982–1999). However, the potential influence of arid, transitional, and humid regions on CDHW characteristics varies between the continents in a warming climate. Such inter-regime and inter-continental heterogeneities may arise due to the non-uniformity in land surface fluxes (hydrological changes) over the water-limited and energy-limited regions under global warming (Kumar et al., 2016). Besides, an increase in the spatiotemporal changes in the magnitude and variability of seasonal precipitation and evaporation (Konapala et al., 2020) can amplify the CDHW event characteristics in the recent warmer period. Furthermore, these heterogeneous impacts can also be attributed to the spatiotemporal variation in soil moisture and wind speed under a changing climate that plays a significant role in modulating the land-atmospheric interactions leading to increases in frequency, duration, and severity of CDHW events (McVicar et al., 2012; Schwingshackl et al., 2017; Seneviratne et al., 2010).

4. Discussion and Concluding Remarks

The impact of compound drought and heatwave events results in more significant socio-economic damage compared to individual events. This study investigated compound drought and heatwave characteristics, such as frequency, duration, severity, and spatial extent based on a relatively warmer recent (2000–2016) and a past period (1983–1999). The analysis is performed using three different combinations of observed and reanalysis-based data sets to examine if the results are independent of the choice of data sources. In all three data sets, a significant increase in drought-related heat waves and the corresponding spatial extent is noted in the (warmer) recent period. Besides, frequency, duration, and severity of CDHW events have increased substantially during the recent period. Our results highlight the regional amplifications of drought and heatwave characteristics, which are often attributed to anthropogenic climate change (Erfanian et al., 2017;

Griffin & Anchukaitis, 2014; Shao et al., 2018; Tingley & Huybers, 2013; Williams et al., 2015). The asymmetric influence of warming was also revealed by the latitudinal variations in CDHW event metrics and the associated temporal skewness in such variations with the NH witnessing more amplification in the recent (2000–2016) warmer climate. The positive influence of warming on the CDHW event metrics is more prominent in arid regions of the globe, and most importantly, the arid regions located in the continents of Asia, Europe, Australia, and North America. However, the CDHW characteristics over the arid regions located in Africa did not witness notable changes, which may be due to relatively greater (10%–20%) amount of precipitation in the recent decade (2000–2009) as compared to the past decade (1990–1999) across some stations located in the arid regimes within the continent (Nicholson et al., 2018). A significant shift in CDHW metrics over global arid lands highlights the potential influence of background aridity and the dominant role of incoming energy and soil moisture variations in modulating the evaporation and intensification of CDHW events in a warmer climate (Seneviratne et al., 2010). Data-related inconsistencies in the results are mainly noted across the humid regions, especially in the equatorial belt.

The broad implication of our study is relevant to stakeholders associated with water resources (Mukherjee et al., 2020), agriculture (Lu et al., 2018; Zampieri et al., 2017), and health science-related disciplines. The results from this study are particularly useful for CDHW impact assessment on health risk, crop loss, and energy demands that are often neglected by the decision-makers and stakeholders. Besides, adequate measures can be implemented by developing suitable forecasting tools to provide early warnings related to CDHW events.

The quantification of the local to regional scale CDHW events are seldom challenging due to uncertainty associated with available data (Mukherjee et al., 2020; Trenberth et al., 2014), and differences in the evolution of drought and heatwaves at different spatial scales and temporal resolutions (Mukherjee et al., 2020). For example, monthly temperature anomalies compromise the daily variation of HW events; on the other hand, the precipitation-based drought indicators potentially ignore the influence of temperature on droughts under warming scenarios. Furthermore, spatiotemporal changes and heterogeneity in the CDHW event characteristics are often associated with large scale teleconnections (Hao et al., 2018b; Mukherjee et al., 2020), variations in soil moisture (Schwingshackl et al., 2017), magnitude and variability of seasonal precipitation and evaporation (Konapala et al., 2020), as well as anthropogenic warming (Konapala et al., 2020; Zscheischler et al., 2018). Therefore, integrating relative contributions from these influencing factors in a more comprehensive manner can advance our understanding of the evolution of compound events.

Data Availability Statement

We are thankful for the data provided by the NOAA Climate Prediction Centre (NOAA CPC; http://www.cpc.ncep.noaa.gov/), Global Precipitation Climatology Center (GPCC; https://www.dwd.de/EN/ourservices/gpcc/gpcc.html), and high-resolution European Centre for Medium-Range Weather Forecasts Reanalysis 5 (ERA5).

Acknowledgments
This study was supported by the National Science Foundation (NSF) award # 1653841. Additionally, we thank editor, Dr. Valeriy Ivanov, and the reviewers for their valuable and constructive feedback to improve the original manuscript.

References

Barriopedro, D., Gouveia, C. M., Trigo, R. M., & Wang, L. (2012). The 2009/10 drought in China: Possible causes and impacts on vegetation. *Journal of Hydrometeorology*, *13*(4), 1251–1267. https://doi.org/10.1175/JHM-D-11-074.1

Barrow, C. J. (1992). World atlas of desertification (United Nations Environment Programme). In N. Middleton, & D. S. G. Thomas (Eds.), Land degradation & development (3, pp. 249–249). London, UK: Edward Arnold. https://doi.org/10.1002/ldr.3400030407

Budyko, M. I., & Mikhail, I. (1971). *Climate and life*. Elsevier. Retrieved from https://agris.fao.org/agris-search/search.do?recordID=US201300494263.

Chen, X., Alimohammadi, N., & Wang, D. (2013). Modeling interannual variability of seasonal evaporation and storage change based on the extended Budyko framework. *Water Resources Research*, *49*(9), 6067–6078. https://doi.org/10.1002/wrcr.20493

Cherlet, M., Hutchinson, C., Reynolds, J., Hill, J., Sommer, S., & Von Maltitz, G. (2018). *World atlas of desertification: Rethinking land degradation and sustainable land management*. Publications Office of the European Union.

Cowan, T., Purich, A., Perkins, S., Pezza, A., Boschat, G., & Sadler, K. (2014). More frequent, longer, and hotter heat waves for Australia in the twenty-first century. *Journal of Climate*, *27*(15), 5851–5871. https://doi.org/10.1175/JCLI-D-14-00092.1

Diaz, H. F., & Wahl, E. R. (2015). Recent California water year precipitation deficits: A 440-year perspective. *Journal of Climate*, *28*(12), 4637–4652. https://doi.org/10.1175/JCLI-D-14-00774.1

D'Ippoliti, D., Michelozzi, P., Marino, C., de'Donato, F., Menne, B., Katsouyanni, K., et al. (2010). The impact of heat waves on mortality in 9 European cities: Results from the EuroHEAT project. *Environmental Health*, *9*(1), 37. https://doi.org/10.1186/1476-069X-9-37

Erfanian, A., Wang, G., & Fomenko, L. (2017). Unprecedented drought over tropical South America in 2016: Significantly under-predicted by tropical SST. *Scientific Reports*, *7*(1), 5811. https://doi.org/10.1038/s41598-017-05373-2

Fink, A. H., Brücher, T., Krüger, A., Leckebusch, G. C., Pinto, J. G., & Ulbrich, U. (2004). The 2003 European summer heatwaves and drought -synoptic diagnosis and impacts. *Weather*, *59*(8), 209–216. https://doi.org/10.1256/wea.73.04

Fischer, E. M., & Knutti, R. (2015). Anthropogenic contribution to global occurrence of heavy-precipitation and high-temperature extremes. *Nature Climate Change*, *5*(6), 560–564. https://doi.org/10.1038/nclimate2617

Fu, Q., & Feng, S. (2014). Responses of terrestrial aridity to global warming. *Journal of Geophysical Research: Atmosphere*, *119*(13), 7863–7875. https://doi.org/10.1002/2014JD021608

Greve, P., Roderick, M. L., Ukkola, A. M., & Wada, Y. (2019). The aridity index under global warming. *Environmental Research Letters*, *14*(12), 124006. https://doi.org/10.1088/1748-9326/ab5046

Griffin, D., & Anchukaitis, K. J. (2014). How unusual is the 2012–2014 California drought? *Geophysical Research Letters*, *41*(24), 9017–9023. https://doi.org/10.1002/2014GL062433

Hao, Z., Hao, F., Singh, V. P., & Zhang, X. (2018a). Changes in the severity of compound drought and hot extremes over global land areas. *Environmental Research Letters*, *13*(12), 124022. https://doi.org/10.1088/1748-9326/aaee96

Hao, Z., Hao, F., Singh, V. P., & Zhang, X. (2018b). Quantifying the relationship between compound dry and hot events and El Niño–southern Oscillation (ENSO) at the global scale. *Journal of Hydrology*, *567*, 332–338. https://doi.org/10.1016/j.jhydrol.2018.10.022

Ionita, M., Tallaksen, L., Kingston, D., Stagge, J., Laaha, G., Van Lanen, H., et al. (2017). The European 2015 drought from a climatological perspective. *Hydrology and Earth System Sciences*, *21*, 1397–1419. https://doi.org/10.5194/hess-21-1397-2017

Karl, T. R., & Trenberth, K. E. (2003). Modern global climate change. *Science*, *302*(5651), 1719–1723. https://doi.org/10.1126/science.1090228

Keellings, D., & Waylen, P. (2014). Increased risk of heat waves in Florida: Characterizing changes in bivariate heat wave risk using extreme value analysis. *Applied Geography*, *46*, 90–97. https://doi.org/10.1016/j.apgeog.2013.11.008

Kendall, M. G. (1948). *Rank correlation methods*. Oxford, UK: Griffin.

Konapala, G., & Mishra, A. (2020). Quantifying climate and catchment control on hydrological drought in the continental United States. *Water Resources Research*, *56*(1), e2018WR024620. https://doi.org/10.1029/2018WR024620

Konapala, G., Mishra, A. K., Wada, Y., & Mann, M. E. (2020). Climate change will affect global water availability through compounding changes in seasonal precipitation and evaporation. *Nature Communications*, *11*(1), 3044. https://doi.org/10.1038/s41467-020-16757-w

Kong, Q., Guerreiro, S. B., Blenkinsop, S., Li, X.-F., & Fowler, H. J. (2020). Increases in summertime concurrent drought and heatwave in Eastern China. *Weather and Climate Extremes*, *28*, 100242. https://doi.org/10.1016/j.wace.2019.100242

Kumar, S., Zwiers, F., Dirmeyer, P. A., Lawrence, D. M., Shrestha, R., & Werner, A. T. (2016). Terrestrial contribution to the heterogeneity in hydrological changes under global warming. *Water Resources Research*, *52*(4), 3127–3142. https://doi.org/10.1002/2016WR018607

Leonard, M., Westra, S., Phatak, A., Lambert, M., van den Hurk, B., McInnes, K., et al. (2014). A compound event framework for understanding extreme impacts. *WIREs Climate Change*, *5*(1), 113–128. https://doi.org/10.1002/wcc.252

Lewis, S. C., & Karoly, D. J. (2013). Anthropogenic contributions to Australia's record summer temperatures of 2013. *Geophysical Research Letters*, *40*(14), 3705–3709. https://doi.org/10.1002/grl.50673

Liu, X., He, B., Guo, L., Huang, L., & Chen, D. (2020). Similarities and differences in the mechanisms causing the European summer heatwaves in 2003, 2010, and 2018. *Earth's Future*, *8*(4), e2019EF001386. https://doi.org/10.1029/2019EF001386

Lough, J. M. (1995). Temperature variations in a tropical-subtropical environment: Queensland, Australia, 1910–1987. *International Journal of Climatology*, *15*(1), 77–95. https://doi.org/10.1002/joc.3370150109

Lu, Y., Hu, H., Li, C., & Tian, F. (2018). Increasing compound events of extreme hot and dry days during growing seasons of wheat and maize in China. *Scientific Reports*, *8*(1), 16700. https://doi.org/10.1038/s41598-018-34215-y

Mann, H. B. (1945). Nonparametric tests against trend. *Econometrica*, *13*(3), 245–259. https://doi.org/10.2307/1907187

Manning, C., Widmann, M., Bevacqua, E., Van Loon, A. F., Maraun, D., & Vrac, M. (2018). Soil moisture drought in Europe: A compound event of precipitation and potential evapotranspiration on multiple time scales. *Journal of Hydrometeorology*, *19*(8), 1255–1271. https://doi.org/10.1175/JHM-D-18-0017.1

Mazdiyasni, O., & AghaKouchak, A. (2015). Substantial increase in concurrent droughts and heatwaves in the United States. *Proceedings of the National Academy of Sciences*. *112*, 11484–11489. https://doi.org/10.1073/pnas.1422945112

McVicar, T. R., Roderick, M. L., Donohue, R. J., Li, L. T., Van Niel, T. G., Thomas, A., et al. (2012). Global review and synthesis of trends in observed terrestrial near-surface wind speeds: Implications for evaporation. *Journal of Hydrology*, *416*(417), 182–205. https://doi.org/10.1016/j.jhydrol.2011.10.024

Meehl, G. A., & Tebaldi, C. (2004). More intense, more frequent, and longer lasting heat waves in the 21st century. *Science*, *305*(5686), 994–997. https://doi.org/10.1126/science.1098704

Meehl, G. A., Washington, W. M., Ammann, C. M., Arblaster, J. M., Wigley, T. M. L., & Tebaldi, C. (2004). Combinations of natural and Anthropogenic forcings in twentieth-century climate. *Journal of Climate*, *17*(19), 3721–3727. https://doi.org/10.1175/1520-0442(2004)017<3721:CONAAF>2.0.CO;2

Miralles, D. G., Gentine, P., Seneviratne, S. I., & Teuling, A. J. (2019). Land–atmospheric feedbacks during droughts and heatwaves: State of the science and current challenges. *Annals of the New York Academy of Sciences*, *1436*(1), 19–35. https://doi.org/10.1111/nyas.13912

Mishra, A. K., & Singh, V. P. (2010). A review of drought concepts. *Journal of Hydrology*, *391*(1), 202–216. https://doi.org/10.1016/j.jhydrol.2010.07.012

Mitchell, D., Heaviside, C., Vardoulakis, S., Huntingford, C., Masato, G., Guillod, B. P., et al. (2016). Attributing human mortality during extreme heat waves to anthropogenic climate change. *Environmental Research Letters*, *11*(7), 074006. https://doi.org/10.1088/1748-9326/11/7/074006

Mukherjee, S., Ashfaq, M., & Mishra, A. K. (2020). Compound drought and heatwaves at a global scale: The role of natural climate variability-associated synoptic patterns and land-surface energy budget anomalies. *Journal of Geophysical Research: Atmosphere*, *125*(11), e2019JD031943. https://doi.org/10.1029/2019JD031943

Mukherjee, S., Mishra, A., & Trenberth, K. E. (2018). Climate change and drought: A perspective on drought indices. *Current Climate Change Reports*, *4*, 145–163. https://doi.org/10.1007/s40641-018-0098-x

Nicholson, S. E., Funk, C., & Fink, A. H. (2018). Rainfall over the African continent from the 19th through the 21st century. *Global and Planetary Change*, *165*, 114–127. https://doi.org/10.1016/j.gloplacha.2017.12.014

Perkins, S. E., Alexander, L. V., & Nairn, J. R. (2012). Increasing frequency, intensity and duration of observed global heatwaves and warm spells. *Geophysical Research Letters*, *39*(L20174). https://doi.org/10.1029/2012GL053361

Sankarasubramanian, A., Wang, D., Archfield, S., Reitz, M., Vogel, R. M., Mazrooei, A., & Mukhopadhyay, S. (2020). HESS opinions: Beyond the long-term water balance: Evolving Budyko's supply–demand framework for the Anthropocene towards a global synthesis of land-surface fluxes under natural and human-altered watersheds. *Hydrology and Earth System Sciences*, *24*(4), 1975–1984. https://doi.org/10.5194/hess-24-1975-2020

Schwingshackl, C., Hirschi, M., & Seneviratne, S. I. (2017). Quantifying spatiotemporal variations of soil moisture control on surface energy balance and near-surface air temperature. *Journal of Climate*, *30*(18), 7105–7124. https://doi.org/10.1175/JCLI-D-16-0727.1

Seneviratne, S. I., Corti, T., Davin, E. L., Hirschi, M., Jaeger, E. B., Lehner, I., et al. (2010). Investigating soil moisture–climate interactions in a changing climate: A review. *Earth-Science Reviews*, *99*(3), 125–161. https://doi.org/10.1016/j.earscirev.2010.02.004

Shao, D., Chen, S., Tan, X., & Gu, W. (2018). Drought characteristics over China during 1980–2015. *International Journal of Climatology*, *38*(9), 3532–3545. https://doi.org/10.1002/joc.5515

Sun, Q., Miao, C., Duan, Q., Ashouri, H., Sorooshian, S., & Hsu, K.-L. (2018). A review of global precipitation data sets: Data sources, estimation, and intercomparisons. *Reviews of Geophysics*, *56*(1), 79–107. https://doi.org/10.1002/2017RG000574

Sutanto, S. J., Vitolo, C., Di Napoli, C., D'Andrea, M., & Van Lanen, H. A. J. (2020). Heatwaves, droughts, and fires: Exploring compound and cascading dry hazards at the Pan-European scale. *Environment International*, *134*, 105276. https://doi.org/10.1016/j.envint.2019.105276

Teuling, A. J., Loon, A. F. V., Seneviratne, S. I., Lehner, I., Aubinet, M., Heinesch, B., et al. (2013). Evapotranspiration amplifies European summer drought. *Geophysical Research Letters*, *40*(10), 2071–2075. https://doi.org/10.1002/grl.50495

Thornthwaite, C. W. (1948). An approach toward a rational classification of climate. *Geographical Review*, *38*(1), 55–94. https://doi.org/10.2307/210739

Tingley, M. P., & Huybers, P. (2013). Recent temperature extremes at high northern latitudes unprecedented in the past 600 years. *Nature*, *496*(7444), 201–205. https://doi.org/10.1038/nature11969

Trenberth, K. E., Dai, A., van der Schrier, G., Jones, P. D., Barichivich, J., Briffa, K. R., & Sheffield, J. (2014). Global warming and changes in drought. *Nature Climate Change*, *4*(1), 17–22. https://doi.org/10.1038/nclimate2067

Unkašević, M., & Tošić, I. (2013). Trends in temperature indices over Serbia: Relationships to large-scale circulation patterns. *International Journal of Climatology*, *33*(15), 3152–3161. https://doi.org/10.1002/joc.3652

Wang, H., & He, S. (2015). The North China/Northeastern Asia severe summer drought in 2014. *Journal of Climate*, *28*(17), 6667–6681. https://doi.org/10.1175/JCLI-D-15-0202.1

Wang, D., & Tang, Y. (2014). A one-parameter Budyko model for water balance captures emergent behavior in darwinian hydrologic models. *Geophysical Research Letters*, *41*(13), 4569–4577. https://doi.org/10.1002/2014GL060509

Webb, R., Rosenzweig, C. E., & Levine, E. R. (2000). *Global soil texture and derived water-holding capacities*. ORNL DAAC. https://doi.org/10.3334/ORNLDAAC/548

Wells, N., Goddard, S., & Hayes, M. J. (2004). A self-calibrating Palmer Drought Severity Index. *Journal of Climate*, *17*(12), 2335–2351. https://doi.org/10.1175/1520-0442(2004)017<2335:ASPDSI>2.0.CO;2

Williams, A. P., Seager, R., Abatzoglou, J. T., Cook, B. I., Smerdon, J. E., & Cook, E. R. (2015). Contribution of anthropogenic warming to California drought during 2012–2014. *Geophysical Research Letters*, *42*(16), 6819–6828. https://doi.org/10.1002/2015GL064924

Witte, J. C. D. (2011). NASA A-Train and Terra observations of the 2010 Russian wildfires. *Atmospheric Chemistry and Physics*, *11*, 9287–9301. https://doi.org/10.5194/acp-11-9287-2011

Wu, X., Hao, Z., Hao, F., Li, C., & Zhang, X. (2019). Spatial and temporal variations of compound droughts and hot extremes in China. *Atmosphere*, *10*(2), 95. https://doi.org/10.3390/atmos10020095

Wu, Z., Lin, H., Li, J., Jiang, Z., & Ma, T. (2012). Heat wave frequency variability over North America: Two distinct leading modes. *Journal of Geophysical Research*, *117*(D2). https://doi.org/10.1029/2011JD016908

Ye, L., Shi, K., Xin, Z., Wang, C., & Zhang, C. (2019). Compound droughts and heat waves in China. *Sustainability*, *11*(12), 3270. https://doi.org/10.3390/su11123270

Zampieri, M., Ceglar, A., Dentener, F., & Toreti, A. (2017). Wheat yield loss attributable to heat waves, drought and water excess at the global, national and subnational scales. *Environmental Research Letters*, *12*(6), 064008. https://doi.org/10.1088/1748-9326/aa723b

Zheng, H., Yang, Z.-L., Lin, P., Wei, J., Wu, W.-Y., Li, L., et al. (2019). On the sensitivity of the precipitation partitioning into evapotranspiration and runoff in land surface parameterizations. *Water Resources Research*, *55*(1), 95–111. https://doi.org/10.1029/2017WR022236

Zscheischler, J., Westra, S., van den Hurk, B. J. J. M., Seneviratne, S. I., Ward, P. J., Pitman, A., et al. (2018). Future climate risk from compound events. *Nature Climate Change*, *8*(6), 469–477. https://doi.org/10.1038/s41558-018-0156-3